Journal of Chromatography A, 1370 (2014) 216–229

Contents lists available at ScienceDirect

Journal of Chromatography A

journal homepage: www.elsevier.com/locate/chroma

# Multivariate analysis of mainstream tobacco smoke particulate phase by headspace solid-phase micro extraction coupled with comprehensive two-dimensional gas chromatography–time-of-flight mass spectrometry☆

Michał Brokl[a], Louise Bishop[b], Christopher G. Wright[b], Chuan Liu[b], Kevin McAdam[b], Jean-François Focant[a,*]

[a] CART – Chemistry Department, Organic & Biological Analytical Chemistry, University of Liège, Liège, Belgium
[b] Group Research and Development, British American Tobacco, Regents Park Road, Southampton SO15 8TL, UK

ARTICLE INFO

*Article history:*
Received 29 August 2014
Received in revised form 16 October 2014
Accepted 18 October 2014
Available online 24 October 2014

*Keywords:*
Solid-phase microextraction (SPME)
Comprehensive two-dimensional gas chromatography (GC × GC)
Central composite design (CCD)
Mainstream tobacco smoke particulate phase (PP)
Principal component analysis (PCA)
Fisher ratio

ABSTRACT

A method involving headspace solid-phase microextraction (HS-SPME) and comprehensive two-dimensional gas chromatography (GC × GC) coupled to time-of-flight mass spectrometry (TOFMS) was developed and applied to evaluate profiles of volatile compounds present in mainstream tobacco smoke particulate matter trapped on glass fiber filters. Six SPME fibers were tested for the extraction capacities toward selected compounds, showing the best results for the polyacrylate fiber. The optimization of the extraction conditions was carried out using multivariate response surface methodology. Two cigarette types differing in a filter design were analyzed using optimized conditions. A template was built in order to generate comprehensive chemical information, which conceded obtaining consistent information across 24 chromatograms. Principal component analysis (PCA) allowed a clear differentiation of the studied cigarette types. Fisher ratio analysis allowed identification of compounds responsible for the chemical differences between the cigarette samples. Of the selected 143 most important ones, 134 analytes were reduced by the active carbon filter, while for nine, classical cellulose acetate filter was more efficient.


## 1. Introduction

Tobacco smoke is an aerosol containing an extremely complex mixture of chemicals [1]. It consists of liquid/solid droplets, called the particulate phase (PP), suspended in a mixture of gases and semi-volatiles – the vapor phase (VP). Although the majority (95%) of whole cigarette smoke is gaseous phase by weight, with the remainder (5%) being particulates [2], the latter part contains most of the 6000+ identified compounds [3]. Based on gas chromatographic (GC) scans, various investigators have estimated that for each component identified in tobacco smoke there were 5–20 components present at extremely low levels that have not yet been identified, and the total number of tobacco smoke components might reach up to 100,000 [4].

The exhaustive analysis of such complex PP samples is thus a very difficult task, not only because of the number of analytes expected to be present, but also because of the large dynamic range to be considered. One-dimensional gas chromatography (1DGC) has been used for the analysis of tobacco smoke since the early days of the technique. However, due to limitations related to peak capacity and sensitivity, most 1DGC-based methods focus on a relatively small proportion of target analytes. Over the last few years 1DGC was used to assess volatile organic compounds [5–8], polycyclic aromatic hydrocarbons (PAHs) [9,10], carbonyls [11,12], pyridines [13], phenolic compounds [14], or nicotine-related alkaloids [15,16] in cigarette smoke. Comprehensive two-dimensional gas chromatography (GC × GC) is a technique that has been applied for over 20 years to the analysis of complex mixtures [17–20].

☆ Presented at 38th International Symposium on Capillary Chromatography and 11th GC × GC Symposium, 18–23 May 2014, Riva del Garda, Italy.

* Corresponding author at: University of Liège, Chemistry Department – CART, Organic & Biological Analytical Chemistry, Allée du 6 Août B6c, B-4000 Liège, Belgium. Tel.: +32 04 366 35 31; fax: +32 04 366 43 87.
*E-mail address:* JF.Focant@ulg.ac.be (J.-F. Focant).

http://dx.doi.org/10.1016/j.chroma.2014.10.057
0021-9673/

It is generally accepted as a more powerful tool than 1DGC as it offers increased separation capacity due to consecutive separations performed on two orthogonal column phases, higher dimensional structure–retention relationships, and improved signal-to-noise ratio (S/N) that greatly enhances sensitivity. GC × GC coupled to time-of-flight mass spectrometry (TOFMS) has been used successfully for the analysis of tobacco smoke from hand-rolled cigarettes [21], analysis of basic and acidic fractions of solvent refined tobacco smoke [22,23], complex hydrocarbons in the non-polar neutral fraction of cigarette smoke condensates [24], and recently for the analysis of liquid and dynamic headspace extraction of mainstream tobacco smoke PP [19]. Non-scanning TOFMS was used because of the high acquisition rate such a mass analyzer can reach while ensuring the spectral continuity required for efficient MS data deconvolution of overlapping chromatographic peaks. Deconvoluted ion currents (DICs) therefore add-up to the two GC × GC dimensions, further enhancing the separation power of the technique [25].

Solid-phase microextraction (SPME) is a rapid, solvent-free, and sensitive method of extraction based on the sorption of analytes present in a sample or in its headspace (HS) by a thin film of an extracting phase immobilized over the surface of a fused-silica fiber [26]. Since its introduction by Arthur and Pawliszyn in early 1990s [27] it has found a wide usage for the analysis of volatile and semi-volatile compounds in a broad variety of matrices [28–30]. In tobacco and tobacco smoke studies, SPME has been used to assess phenolic compounds in cigarette smoke condensate [31], tobacco additives [32–34], volatiles in tobacco [35], and tobacco smoke [7,8], various alkaloids present in tobacco [36], acetates in tobacco [37], acetaldehyde in mainstream tobacco smoke [38], and free-base nicotine associated with the particulate phase portion of mainstream cigarette smoke [39]. Important parameters affecting SPME methodology for tobacco and tobacco smoke analysis include, among others, the extraction time, extraction temperature or the type of the fiber employed. Optimization of extraction conditions can be carried out by univariate approaches, where each factor is studied separately [7,34,35], or using a multivariate experimental design strategy [40], that allows for simultaneous variation of all evaluated factors. The multivariate approach requires fewer experimental runs and makes it easier to distinguish possible interactions among the factors, that would not be possible to detect using traditional methods [41].

In the present work, a HS-SPME GC × GC TOFMS method was developed for the analysis of mainstream tobacco smoke PP volatile and semi-volatile components from different types of cigarettes using a multivariate optimization strategy for the SPME procedure. A factorial design and response surface methodology were used to evaluate the effects of extraction time and extraction temperature on the extraction efficiency of seven selected representative compounds, measured as peak area. The developed method was applied for statistical comparison of two cigarette types that differed only in a filter construction. The first filter type was made of cellulose acetate and the second type was a two section filter, the first section made of cellulose acetate and the second made from 45 mg high activity carbon distributed randomly within cellulose acetate fibers. Active carbons have been demonstrated to be broad general adsorbents for volatile and semi-volatile cigarette smoke constituents [42], but limited data are currently available regarding the real chemical impact of such filter on the PP composition. The main objective of the present study was to better elucidate the possible differences between these chemical compositions. The HS-SPME GC × GC TOFMS data were treated using a Fisher ratio method [43] in order to highlight the components that statistically differ among sample types.

## 2. Materials and methods

### 2.1. Analytical reagents and supplies

44 mm glass fiber filter pads (Cambridge filter pads) were purchased from Borgwaldt (Germany). Pyridine, styrene, phenol, ethylbenzene, naphthalene, and quinoline were acquired from Sigma Aldrich (Belgium). An alkane standard solution ($C_8$–$C_{20}$) was purchased from Fluka (Belgium). Commercially available SPME fibers in 23 gauge needle sizes suited for automated analysis – 100 μm and 7 μm polydimethylsiloxane (PDMS-100 and PDMS-7, respectively), 85 μm carboxen/polydimethylsiloxane (CAR/PDMS), 65 μm polydimethylsiloxane/divinylbenzene (PDMS/DVB), 50/30 μm divinylbenzene/carboxen/polydimethylsiloxane (DVB/CAR/PDMS), and 85 μm polyacrylate (PA) were purchased from Sigma Aldrich (Belgium). The fibers were conditioned prior to use according to manufacturer's instructions in a Gerstel (Kortrijk, Belgium) fiber bake out station. A blank test was performed to check for possible carry-over. 20 mL headspace vials, PTFE septa magnetic crimp caps, and an automated SPME holder were obtained from Gerstel (Kortrijk, Belgium).

### 2.2. Samples and sample preparation

3R4F research reference cigarettes were acquired from the University of Kentucky College of Agriculture (Kentucky Tobacco Research & Development Center, USA). A classic 27-mm length cellulose acetate filter cigarettes (coded A) and a 27-mm length two-part filter (15 mm cellulose acetate section at the mouth end and a 12 mm cellulose acetate section containing 55 ± 4 mg of indispersed active carbon at the rod end) cigarettes (coded B) were provided by British American Tobacco (Southampton, UK). A and B cigarettes had a circumference of 24.6 mm and were made up of a 56 mm long tobacco rod containing a US style tobacco blend (tobacco rod density of 235 mg $cm^{-3}$ at a moisture content of 13.5%). The carbon used in this study was a high activity, polymer-based material whose production, composition and performance have been described in detail previously [42]. For each analysis five conditioned cigarettes were smoked and the PP of mainstream smoke was trapped on a 44 mm Cambridge filter pad. Cigarettes and Cambridge filter pads were conditioned for at least 48 h at 60% relative air humidity and 22 °C [44]. Smoke samples were produced using a Borgwaldt RM20 rotary smoking machine (Borgwaldt KC, Inc. USA). Smoking was conducted according to the relevant ISO standards applying a 35 mL puff of 2 s duration taken every 60 s with no blocking of filter ventilation holes [45]. Cigarettes were lit using an electric lighter (Borgwaldt KC, Inc. USA). After smoking, the filter pad was cut into quarters and each quarter was placed in a separate 20 mL headspace vial which was sealed and analyzed immediately after.

### 2.3. Headspace solid-phase microextraction (HS-SPME) procedures

In the preliminary selection, the extraction capacities of all six fibers toward mainstream tobacco smoke volatiles were compared (triplicate analysis per fiber coating). The test system was the mainstream smoke particulate phase of 3R4F cigarettes. This step consisted of exposing the fibers to the sample headspace using arbitrarily established conditions: an incubation time of 10 min at 50 °C and an extraction time of 10 min performed at 50 °C. The fiber was desorbed in a CIS4 Cooled Injection System (Gerstel, Kortrijk, Belgium) using the following temperature program: isothermal period at −20 °C for 0.5 min, a ramp of 12 °C $s^{-1}$ to 250 °C and kept for 2 min. After desorption, the fiber was submitted to 40 min conditioning according to manufacturer's guidelines to eliminate

**Table 1**
Experimental parameters employed for central composite design (CCD).

| Variable | Coded variable | | | | |
|---|---|---|---|---|---|
| | $-\alpha$[a] | −1 | 0 | 1 | $\alpha$[a] |
| Extraction temperature (°C) | 36 | 40 | 50 | 60 | 64 |
| Extraction time (min) | 3 | 5 | 10 | 15 | 17 |

[a] $\alpha = 1.414$.

possible carry-over from previous analysis. For the optimization of HS-SPME conditions, a $2^2$ factorial central composite design (CCD) with four axial points ($\alpha = 1.414$) and four central point replicates, and response surface methodology [41] were used in order to find the optimum values for temperature and extraction time. The variables and levels selected for each variable are listed in Table 1. Twelve duplicated experiments were performed randomly and each run was performed twice. JMP statistical discovery software v.10.0.0 (SAS Institute Inc. USA) was used.

### 2.4. Instrumental analysis

The GC × GC TOFMS system consisted of an Agilent 7890 (Agilent Technologies, Palo Alto, CA, USA) gas chromatograph and a Pegasus 4D TOFMS (LECO, St. Joseph, MI, USA) with quad jet thermal modulator. The first dimension ($^1$D) column was a low-polarity 5% phenyl polysilphenylene-siloxane phase (BPX5; 30 m × 0.25 mm i.d. × 0.25 μm film thickness; SGE International, Victoria, Australia) connected by means of a SilTite™ μ-Union (SGE International, Victoria, Australia) to a second dimension ($^2$D) midpolarity Crossbond® silarylene phase column exhibiting similar selectivity to 50% phenyl/50% dimethyl polysiloxane (Rxi®-17Sil MS; 1.4 m × 0.15 mm i.d. × 0.15 μm film thickness; Restek Corp., Bellefonte, PA, USA). Such a column set was successfully used in a previous study of PP [19]. The $^2$D column was installed in a separate oven located inside the main GC oven, providing more flexible temperature control. The system was equipped with a Gerstel MultiPurpose Sampler (MPS 2XL), SPME option for procedural automation, and the CIS4 Cooled Injection System. The carrier gas was helium at a corrected constant flow rate of 1 mL min$^{-1}$ and the injector was set to splitless mode. In the preliminary selection of fibers, the main oven temperature program comprised an isothermal period at 50 °C for 3 min, a ramp of 3 °C min$^{-1}$ to 185 °C followed by a ramp of 20 °C min$^{-1}$ to 295 °C and a final isothermal period at 295 °C for 6 min. The secondary oven was programmed with a 20 °C offset above the primary oven. The modulation parameters consisted of 6 s modulation period (1 s hot pulse and 2 s cold pulse time) and a temperature offset of 10 °C above the secondary oven. For the sample analysis, due to differences in the cigarette types (3R4F and the two test cigarettes), slightly modified modulation parameters were applied: modulation period of 4 s (0.6 s hot pulse and 1.4 s cold pulse time). Mass spectra were acquired in the range $m/z$ 45–500 at the acquisition rate of 100 spectra s$^{-1}$. The ion source temperature was set at 230 °C and the transfer line temperature was set at 250 °C. The detector voltage was 1500 V and the ionization electron energy (EI source) was set at 70 eV. Samples were acquired using LECO ChromaTOF® software version 4.44.

### 2.5. Data processing

Data processing for fiber selection was performed using the peak table-based LECO ChromaTOF® software version 4.50 applying S/N threshold for automatic peak finding of 1000 and mass threshold of 50. Data processing for multivariate comparison of cigarettes A and B was performed using the pixel-based GC Image™ software package version 2.4a2 (Zoex Corporation, Houston, TX, USA). The Image Investigator™, part of the GC Image™ software package,

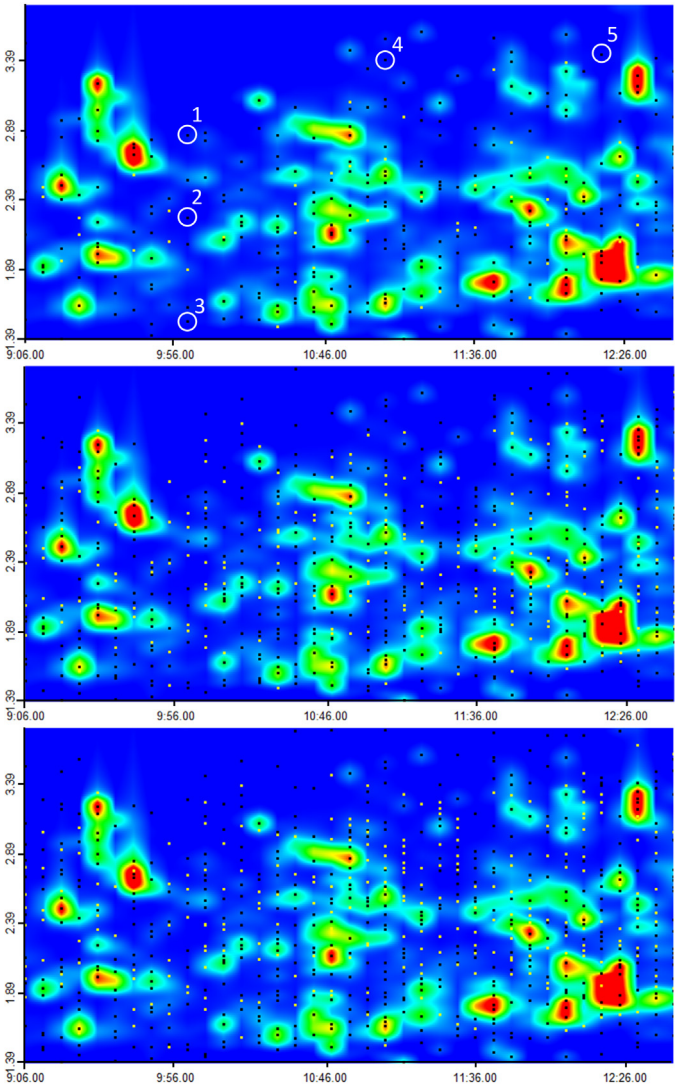


**Fig. 1.** Fragments of chromatogram processed using S/N of 1000 (top), 100 (middle), and 50 (bottom). Black dots represent hits with similarity >70%, yellow ones are hits which could not be identified (similarity <70%). White circles marked from 1 to 5 are hits present at very low abundances yet fulfilling the S/N threshold of 1000; X – compound with the highest peak area in the selected fragment of chromatogram. (For interpretation of the references to color in this text, the reader is referred to the web version of the article.)

was used to analyze multiple chromatograms and examine statistical characteristics and trends. Library searching was carried out using NIST/EPA/NIH Mass Spectral Library (NIST 11) and Wiley Registry of Mass Spectral Data (9th edition), considering a minimum similarity value of 80%. Linear retention indices (LRI) for the first chromatographic dimension were calculated using alkanes present in a sample. Aroma Office $^2$D (Gerstel, Tokyo, Japan) and its LRI database of over 50,000 entries was used for verification of some compound identities. This software allows performing manual searches within selected ± range (±15 in this case) from the calculated LRI value to improve reliability of MS peak identification.

The data processing of the mainstream smoke sample replicates for the two cigarette types (a total of 24 runs; 12 for A and 12 for B) was performed on a matrix of data containing all calculated peak regions (e.g. every single peak found in any of the sample replicates). It consisted of a set of 1100+ compounds (variables) that were detected in each of the analyzed mainstream smoke PP samples. The matrix was submitted to principal component analysis (PCA) with mean-centering pretreatment in order to elucidate

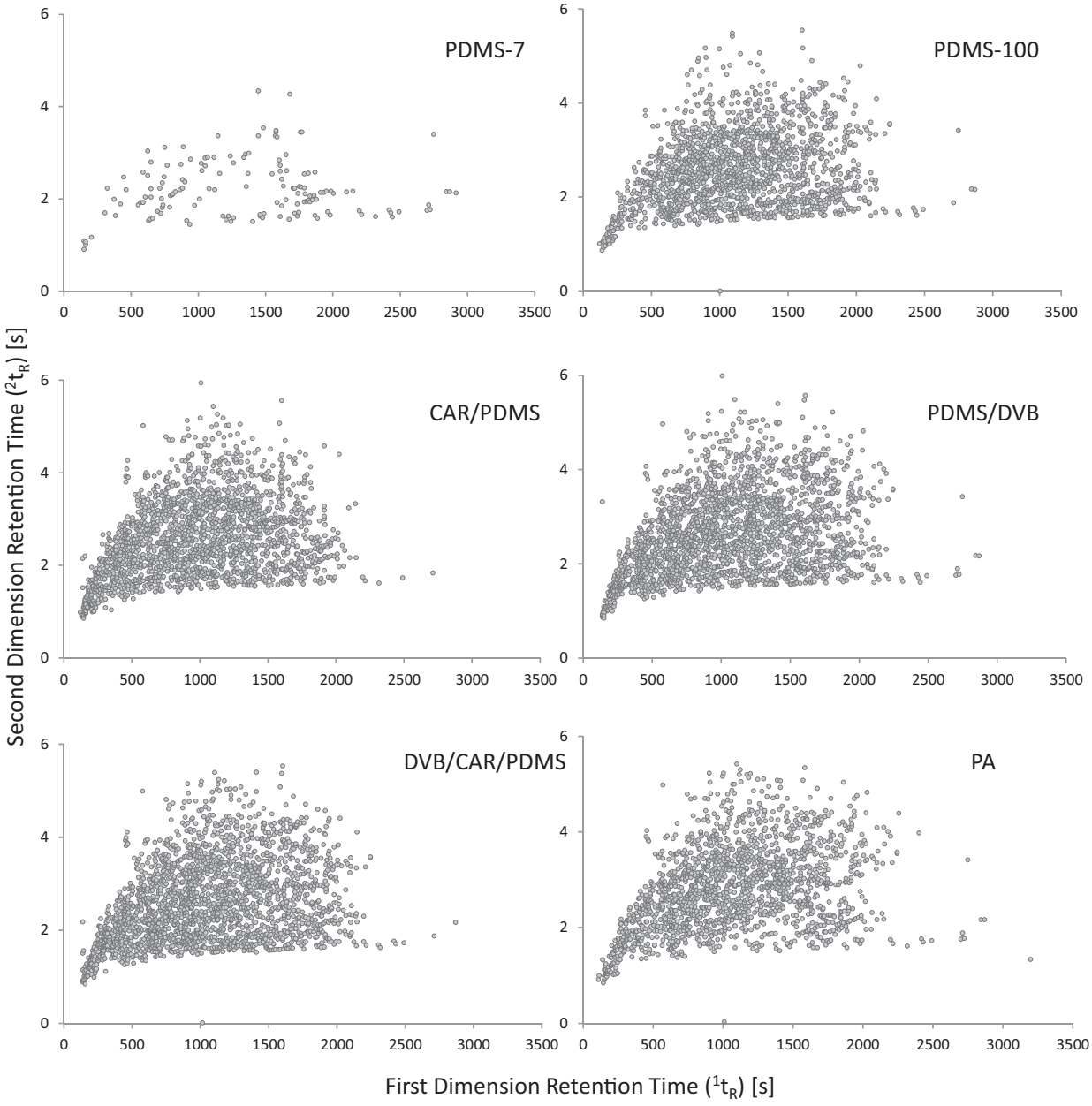


**Fig. 2.** Apex plots showing extraction capacities toward PP volatiles for 6 SPME fibers build from the retention times in two dimensions of selected compounds. Peak tailing, artifacts, column bleeding, and compounds with similarity <80% were filtered out.

clustering tendencies. A 24 × 1170 data matrix was calculated for PCA using chemometrics package Unscrambler® X version 10.3 (Camo, Norway). A singular value decomposition (SVD) algorithm was used as it produces high accuracy results and is best suited for high number of variables datasets [46].

## 3. Results and discussion

### 3.1. SPME fiber selection

The preliminary selection of SPME fibers focused on analysis of 3R4F reference cigarette mainstream smoke as a means to compare of their extraction capacities toward PP volatiles. Each of the six evaluated fiber types was exposed to the headspace over a quarter of a Cambridge filter pad and analyzed under identical conditions. The goal was primarily to maximize the number of detected compounds, but not at the price of producing overloaded chromatograms that would impact peak shapes and mass spectral data quality, which would greatly confound the quality of the subsequent statistical analysis of the samples.

For these reasons, in the peak table-based data processing approach (ChromaTOF®), we decided to sacrifice the number of hits (unverified compounds detected by the peak finding algorithm) in order to improve the overall quality of processed data, thus giving better identification. Fig. 1 shows three fragments of the same chromatogram processed using S/N (based on unique mass signal, not TIC) of 1000, 100, and 50 (top, middle, and bottom, respectively). Each detected hit is marked with a black dot while the yellow ones are hits which could not be identified (their mass spectra library matching was lower than 70%). Chromatograms processed with S/N of 50 and 100 obviously gave higher number of hits than the one with S/N of 1000, but they also gave rise to much higher numbers of unknowns or hits just at the noise level with very poor mass spectra. These hits would anyway be filtered out during the following

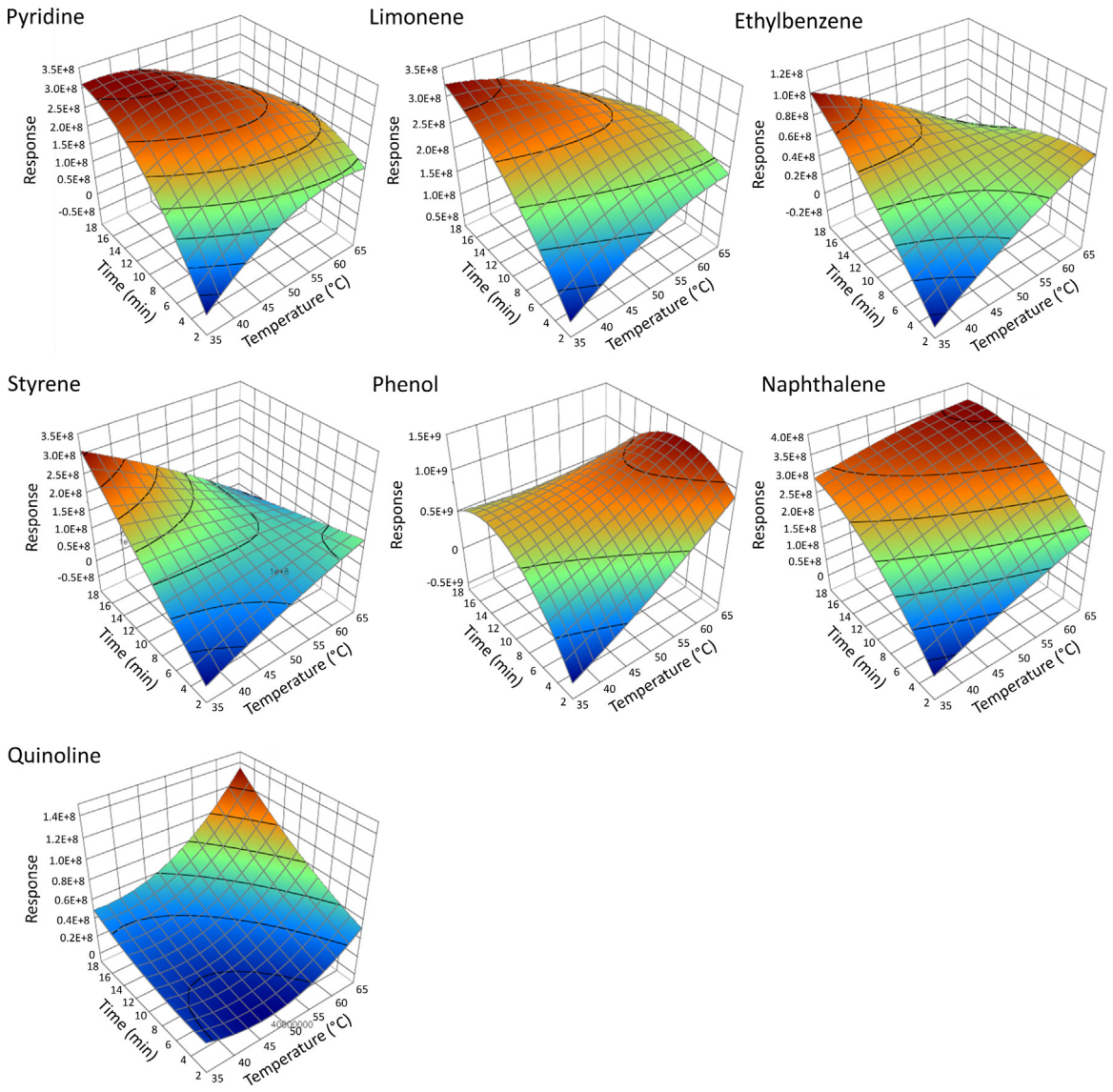


**Fig. 3.** Response surface graphs obtained by central composite design for the seven representative compounds in mainstream tobacco smoke PP in the optimization of the extraction conditions (time and temperature) where the response was a peak area.

manual verification step. The S/N 1000 threshold peaks presented high quality mass spectral data, including analytes present at very low abundances. Fig. 1 (top) shows hits – white circles marked from 1 to 5 – that exhibit S/N of 1858, 1771, 1396, 1369, and 2364, respectively). This clearly shows that, with the selected unique mass S/N threshold, we are able to detect a large range of analytes, including the ones present at very low abundances. When areas of these peaks are compared to areas of the higher abundance compounds present in the same region of the chromatogram (e.g. compound 3 of relative area $250 \times 10^3$ vs. compound *X* of relative area $230 \times 10^6$), it appears that a dynamic range of at least 3 decades is covered by compounds exhibiting good MS data. Results obtained after automated peak finding were further manually filtered for column bleeding, artifacts, and hits with mass spectral similarities lower than 800. Retention time values (first ($^1t_R$) and second ($^2t_R$) dimensions) of compounds after filtering were used to build apex plots that were used for fiber selection and are shown in Fig. 2.

The number of detected compounds for PDMS-7, PDMS-100, CAR/PDMS, PDMS/DVB, DVB/CAR/PDMS, and PA fiber coatings were of 148, 1542, 1782, 1967, 2049, and 1569, respectively. The use of CAR/PDMS, PDMS/DVB, and DVB/CAR/PDMS, which are adsorbent-type coatings, provided the highest numbers of compounds. The construction of these fibers, made of solid materials suspended into a liquid polymer, improves the enrichment of volatiles on the fiber and produces higher extraction efficiency toward low molecular weight compounds [47]. It however resulted in both overloading of the chromatogram and significant peak broadening in both dimensions. This appeared to have a negative effect on the automated peak finding algorithm of the software that led to multiple entries of the same compound in the processed peak table, despite the S/N threshold. For absorbent-type phases such as PDMS and PA, that are composed principally of liquid polymers, the analyte enrichment (apart of polarity) mainly depends on the thickness of the fiber coating. Therefore, unless a thick phase is used, it is more difficult for these phases to retain small molecular weight analytes [47]. This is clearly seen in the performance of PDMS-7 that showed the lowest number of captured analytes (Fig. 2). Even compared to thicker PDMS-100, PA fiber was able to better extract both polar and non-polar compounds, due to its higher polarity, without

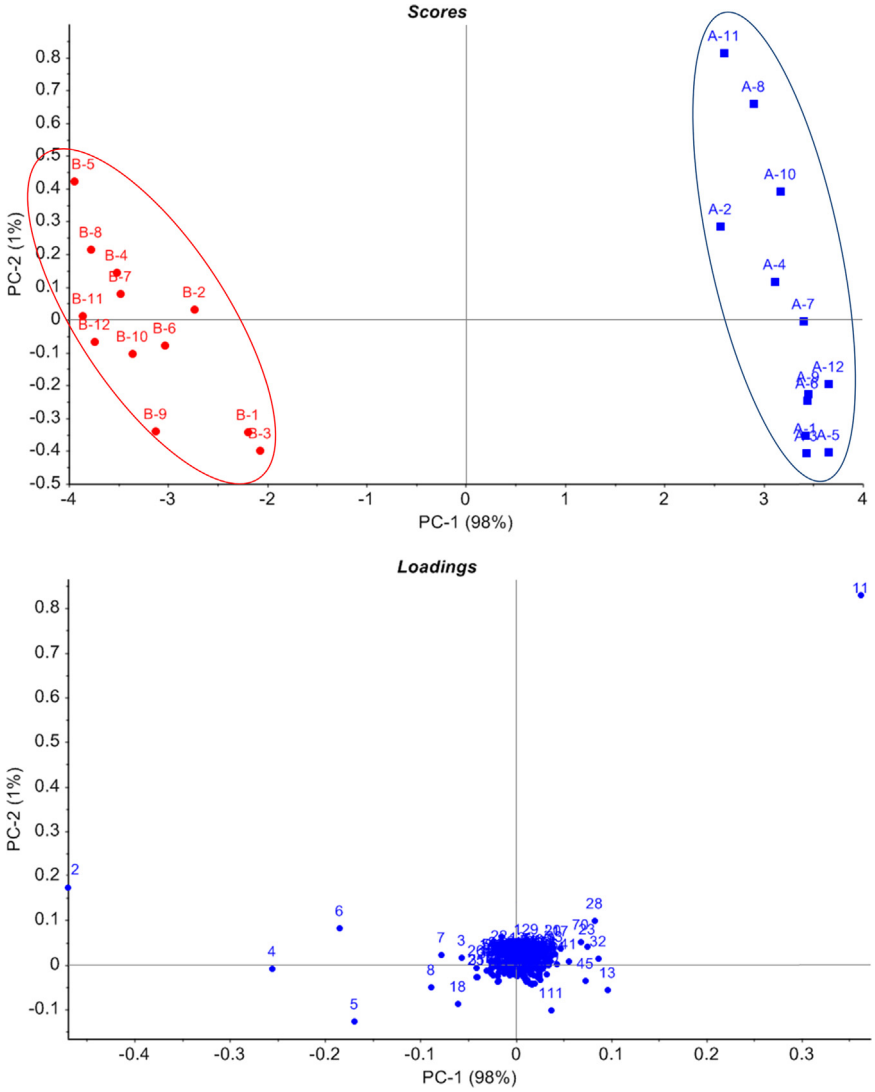


**Fig. 4.** Principal component analysis *score* (top) and *loadings* (bottom) plots for 2 classes of cigarettes.

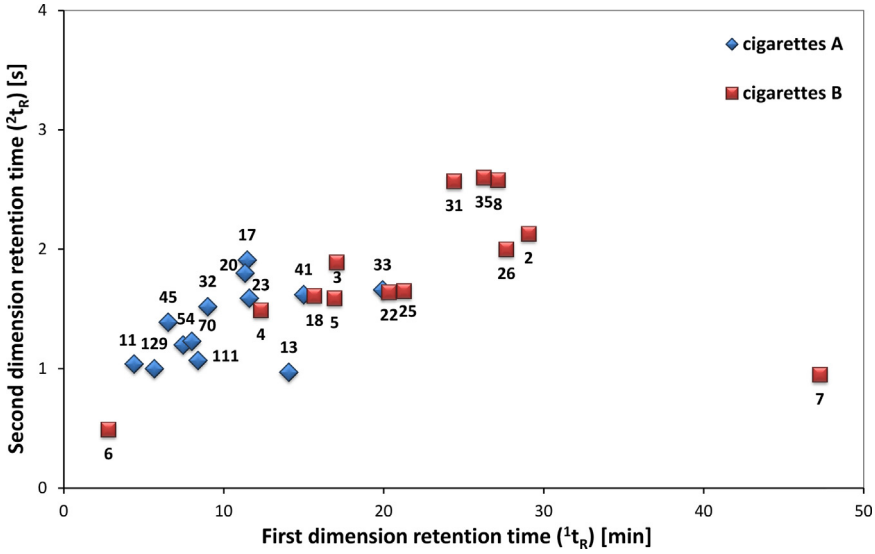


**Fig. 5.** Apex plot of compounds found in PCA *loadings* plot with the biggest influence on the differences between cigarettes A and B. 2 – pyridine, 3-(1-methyl-2-pyrrolidinyl)-, (*S*)-; 3 – phenol, 2-methoxy-; 4 – phenol; 5 – phenol, 3-methyl-; 6 – acetic acid, 7 – neophytadiene; 8 – indole; 11 – 1,2-propanediol; 13 – limonene; 17 – 2-cyclopenten-1-one, 3-methyl-; 18 – phenol, 2-methyl-; 20 – 5-methyl furfural; 22 – phenol, 2,3-dimethyl-; 23 – pyridine, 3-ethenyl-; 25 – phenol, 4-ethyl-; 26 – 2-methoxy-4-vinylphenol; 31 – benzenepropanenitrile; 32 – 2-cyclopenten-1-one, 2-methyl-; 33 – 1-(o-tolyl)-1-propyne; 35 – 1H-Inden-1-one, 2,3-dihydro-; 41 – methylenebenzocyclobutene; 45 – spiro[4.6]undecane; 54 – pyridine, 3-methyl-; 70 – 1-acetoxy-2-propanol; 111 – 1,3,5,7-cyclooctatetraene; 129 – 1,2-propanediol diformate.

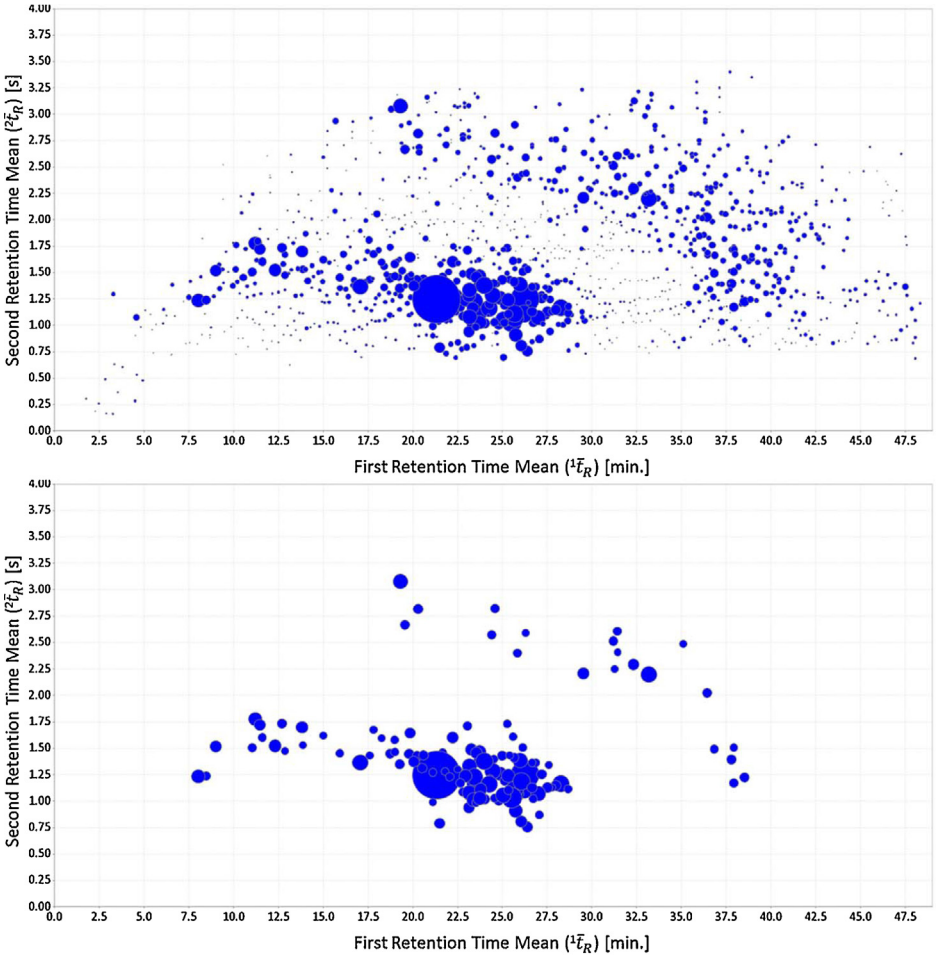


**Fig. 6.** Two-dimensional Fisher ratio plots showing the biggest class-to-class differences between cigarettes A and B for 1170 compounds (top) and for the most influencing ($F > 900$) compounds (bottom).

the overloading issues of the solid material-based fiber coatings. Therefore, PA fiber was selected as it provided clear, non-overloaded chromatograms that included a wider range of analyte polarities.

### 3.2. Optimization of HS-SPME conditions

An experimental design strategy was chosen in order to reduce the number of experiments required to optimize peak areas. To optimize HS-SPME conditions a central composite design (CCD) was conducted to identify the optimum extraction temperature and time. Four replicates of the central point were performed with the objective of estimating experimental error and detecting lack of fit. The matrix for CCD design consisted of 12 duplicated experimental runs performed in random order. A second-degree polynomial model was used including main effects for the two factors – extraction temperature and extraction time, their interaction and their quadratic components. For the purpose of the experimental design, seven representative compounds of various chemical families were selected, based on their significance in tobacco smoke and exhibiting various volatilities and polarities: pyridine, ethylbenzene, styrene, limonene, phenol naphthalene, and quinoline. The aim was to search for extraction time and extraction temperature values (independent variables) for which the peak areas of the afore mentioned compounds (dependent variables) were maximized. The average values from duplicated experiment (in arbitrary units of peak area) and experimental conditions are listed in Table S1 of Supplementary material.

Supplementary material related to this article can be found, in the online version, at http://dx.doi.org/10.1016/j.chroma.2014.10.057.

The analysis of variance (ANOVA) performed to evaluate the model showed the absence of significant lack of fit (meaning, that it adequately describes the functional relationship between the experimental factors and the response variables), and good values for $R^2$ (0.7741 for pyridine, 0.8195 for limonene, 0.7805 for ethylbenzene, 0.7887 for styrene, 0.9072 for phenol, 0.9597 for naphthalene, and 0.9429 for quinoline). These values demonstrated that the proportion of variation in the response was attributed to the model rather than to random error. Fig. 3 shows the response surface graphs obtained in the CCD for the seven selected compounds. The maximized responses for pyridine, limonene, ethylbenzene, and styrene were obtained at lower temperatures and longer extraction times; naphthalene and quinoline needed both higher temperature and longer extraction times to maximize the response, while for phenol this was achieved at higher temperature and approximately 8 min of extraction. Each of these separately modeled responses were processed through a desirability function, rather than combining several elementary responses into a more complex objective function [41]. The overall optimum of extraction conditions, identified by maximized desirability, were an extraction temperature of 40 °C and 15 min extraction time.

**Table 2**
List of tentatively identified compounds exhibiting biggest differences between classes of cigarettes based on Fisher ratio analysis.

| Blob ID | Area name | $^1t_R$ mean [min] | $^2t_R$ mean [s] | LRI | *F* | Peak volume mean (A) $\times 10^6$ | Peak volume mean (B) $\times 10^6$ | Peak volume mean ratio | Vapor pressure at 298 K [Torr] | MW | Chemical class[a] |
|---|---|---|---|---|---|---|---|---|---|---|---|
| 28 | Menthol | 21.33 | 1.25 | 1189 | 6648 | 213.12 | 17.69 | 0.08 | 3.23E−02 | 156 | 10 |
| 499 | Menthyl acetate | 26.28 | 1.25 | 1297 | 3900 | 15.26 | 2.15 | 0.14 | 7.07E−02 | 198 | 11 |
| 847 | Unknown | 25.53 | 1.03 | 1281 | 2712 | 4.45 | 0.62 | 0.14 | – | – | – |
| 811 | Unknown | 25.71 | 1.07 | 1284 | 2436 | 3.53 | 0.56 | 0.16 | – | – | – |
| 474 | 1,4-Methanocycloocta[d]pyridazine, 1,4,4a,5,6,9,10,10a-octahydro-11,11-dimethyl-, (1α,4α,4aα,10aα)- | 26.21 | 1.11 | 1297 | 2376 | 12.14 | 1.97 | 0.16 | 1.07E−02 | 204 | 8 |
| 818 | Unknown | 25.69 | 1.11 | 1284 | 2340 | 5.57 | 0.86 | 0.15 | – | – | – |
| 828 | Unknown | 26.07 | 1.19 | 1293 | 2340 | 2.04 | 0.28 | 0.14 | – | – | – |
| 92 | 3,3-Dimethyl-4-phenylbutene | 24.00 | 1.38 | 1247 | 2316 | 54.91 | 8.02 | 0.15 | 3.60E−04 | 160 | 2 |
| 672 | Unknown | 23.43 | 1.23 | 1235 | 2256 | 8.75 | 1.04 | 0.12 | – | – | – |
| 617 | 1,7-Octadiene, 2,7-dimethyl-3,6-bis(methylene)- | 28.27 | 1.17 | 1342 | 2220 | 6.95 | 1.31 | 0.19 | 1.75E−01 | 162 | 5 |
| 867 | 5-(Propenyl-2)-1,3,7-nonatriene | 24.28 | 1.16 | 1253 | 2220 | 2.05 | 0.25 | 0.12 | – | 162 | 5 |
| 461 | 4-Methyl-1-(2-methylbutyl)benzene | 24.47 | 1.28 | 1257 | 2160 | 11.67 | 1.60 | 0.14 | 1.68E−01 | 162 | 2 |
| 451* | Naphthalene, 1,6-dimethyl- | 33.19 | 2.20 | 1457 | 2136 | 1.94 | 2.37 | 1.22 | 1.59E−02 | 156 | 1 |
| 51 | Benzene, 1-methyl-4-(1-methylethenyl)- | 17.07 | 1.36 | 1098 | 2088 | 89.72 | 7.95 | 0.09 | 8.34E−01 | 132 | 2 |
| 908 | Cyclooctene, 3-(1-methylethenyl)- | 25.07 | 1.06 | 1271 | 2040 | 2.93 | 0.33 | 0.11 | 4.61E−01 | 150 | 3 |
| 548 | Benzene, (1,2,2-trimethyl-3-butenyl)- | 26.00 | 1.38 | 1291 | 1992 | 14.81 | 2.69 | 0.18 | 1.87E−01 | 174 | 2 |
| 848 | Unknown | 27.02 | 1.07 | 1314 | 1992 | 4.41 | 0.73 | 0.17 | – | – | – |
| 788 | Unknown | 23.17 | 1.08 | 1229 | 1980 | 3.28 | 0.34 | 0.10 | – | – | – |
| 216 | 2(3H)-Furanone, 5-acetyldihydro- | 19.31 | 3.08 | 1146 | 1956 | 23.06 | 22.81 | 0.99 | 2.65E−03 | 128 | 12 |
| 905 | 1-Cyclohexyl-1-pentyne | 23.41 | 1.01 | 1234 | 1944 | 3.47 | 0.22 | 0.06 | 2.35E−01 | 150 | 4 |
| 635 | Benzene, 1-(1-methylethenyl)-3-(1-methylethyl)- | 23.17 | 1.33 | 1229 | 1932 | 4.73 | 0.68 | 0.14 | 1.72E−01 | 160 | 2 |
| 242 | Benzene, hexyl- | 24.87 | 1.26 | 1266 | 1836 | 21.45 | 3.10 | 0.14 | 1.25E−01 | 162 | 2 |
| 454 | Benzene, 3-hexenyl- | 23.80 | 1.38 | 1243 | 1836 | 24.62 | 3.74 | 0.15 | 1.53E−01 | 160 | 2 |
| 621 | Unknown | 23.14 | 1.29 | 1229 | 1836 | 8.88 | 1.11 | 0.13 | – | – | – |
| 70 | 1-Acetoxy-2-propanol | 8.02 | 1.23 | 878 | 1824 | 181.62 | 17.42 | 0.10 | 1.42E−01 | 118 | 10 |
| 768 | 1,12-Tridecadiene | 25.75 | 0.91 | 1287 | 1812 | 8.41 | 1.04 | 0.12 | 1.31E−01 | 180 | 5 |
| 825 | Unknown | 25.33 | 1.24 | 1276 | 1812 | 5.82 | 0.87 | 0.15 | – | – | – |
| 995 | Unknown | 23.74 | 1.03 | 1241 | 1800 | 1.64 | 0.14 | 0.09 | – | – | – |
| 309 | 2-Methyl-2,4-pentadien-4-olide | 11.20 | 1.78 | 956 | 1788 | 21.62 | 3.30 | 0.15 | 9.98E−31 | 110 | 12 |
| 706 | Unknown | 22.94 | 1.24 | 1224 | 1704 | 8.60 | 0.79 | 0.09 | – | – | – |
| 480 | 1H-Indene, 2,3-dihydro-1,2-dimethyl- | 23.73 | 1.47 | 1241 | 1692 | 5.35 | 1.07 | 0.20 | 3.52E−01 | 146 | 1 |
| 4 | Phenol | 12.31 | 1.52 | 985 | 1668 | 776.82 | 627.62 | 0.81 | 6.14E−01 | 94 | 13 |
| 964 | Unknown | 23.80 | 1.11 | 1243 | 1632 | 2.52 | 0.22 | 0.09 | – | – | – |
| 325 | Pyrazine, 2-ethenyl-6-methyl- | 13.82 | 1.70 | 1019 | 1608 | 40.68 | 5.19 | 0.13 | 1.78E+00 | 120 | 8 |
| 232 | α,ß,ß-Trimethylstyrene | 23.27 | 1.49 | 1231 | 1596 | 31.82 | 4.64 | 0.15 | 5.16E−02 | 146 | 2 |
| 254* | 2-(2′-Furyl)-5-methylpyrazine | 29.53 | 2.21 | 1371 | 1584 | 25.89 | 28.23 | 1.09 | 4.26E−02 | 160 | 8 |
| 639 | 2-Caren-10-al | 23.36 | 1.16 | 1232 | 1560 | 7.16 | 0.63 | 0.09 | 1.45E−01 | 150 | 9 |
| 52 | 1-Tridecene | 26.07 | 0.81 | 1293 | 1548 | 49.95 | 10.73 | 0.21 | 8.56E−02 | 182 | 5 |
| 540 | Benzene, 1-methyl-2-(1-methyl-2-propenyl)- | 23.55 | 1.46 | 1238 | 1536 | 6.18 | 1.22 | 0.20 | 6.09E−01 | 146 | 2 |
| 32 | 2-Cyclopenten-1-one, 2-methyl- | 9.00 | 1.52 | 902 | 1512 | 236.66 | 25.04 | 0.11 | 2.74E+00 | 96 | 7 |
| 273 | 1H-Indene, 2,3-dimethyl- | 22.22 | 1.60 | 1207 | 1512 | 34.50 | 6.06 | 0.18 | 1.69E−01 | 144 | 1 |
| 47 | Benzaldehyde | 11.46 | 1.72 | 962 | 1488 | 88.79 | 19.05 | 0.21 | 9.74E−01 | 106 | 9 |

Table 2 (*Continued*)

| Blob ID | Area name | $^1t_R$ mean [min] | $^2t_R$ mean [s] | LRI | *F* | Peak volume mean (A) $\times 10^6$ | Peak volume mean (B) $\times 10^6$ | Peak volume mean ratio | Vapor pressure at 298 K [Torr] | MW | Chemical class[a] |
|---|---|---|---|---|---|---|---|---|---|---|---|
| 131 | Benzene, 1-methyl-3-(1-methyl-2-propenyl)- | 21.17 | 1.39 | 1186 | 1488 | 26.78 | 4.25 | 0.16 | 7.10E−01 | 146 | 2 |
| 490 | E-1,8-Dodecadiene | 23.14 | 0.94 | 1229 | 1476 | 10.56 | 0.82 | 0.08 | 9.66E−13 | 166 | 5 |
| 388* | 1-Naphthalenol, 3-methyl- | 32.33 | 2.29 | 1438 | 1464 | 6.31 | 7.24 | 1.15 | 2.72E−04 | 158 | 13 |
| 344 | Benzene, 3-pentenyl-, (Z)- | 20.07 | 1.37 | 1162 | 1452 | 15.62 | 1.68 | 0.11 | 4.34E−01 | 146 | 2 |
| 33 | 1H-Indene, 1-methyl- | 19.85 | 1.64 | 1159 | 1428 | 286.03 | 94.73 | 0.33 | 4.93E−01 | 130 | 1 |
| 810 | Unknown | 27.53 | 1.13 | 1326 | 1404 | 4.75 | 0.83 | 0.17 | – | – | – |
| 116 | 1-Dodecene | 21.50 | 0.79 | 1193 | 1380 | 36.05 | 3.61 | 0.10 | 2.34E−01 | 168 | 5 |
| 120 | Tridecane | 26.40 | 0.76 | 1300 | 1368 | 22.59 | 4.75 | 0.21 | 8.07E−02 | 184 | 6 |
| 734 | Unknown | 28.00 | 1.14 | 1336 | 1356 | 4.37 | 0.82 | 0.19 | – | – | – |
| 970 | 3,4-Octadiene, 7-methyl- | 24.01 | 1.02 | 1247 | 1356 | 1.64 | 0.17 | 0.10 | 5.70E+00 | 124 | 5 |
| 895 | Unknown | 26.67 | 1.13 | 1306 | 1332 | 3.58 | 0.64 | 0.18 | – | – | – |
| 261 | 2-Methylenetricyclo[4.3.1.0(3,8)]dec-4-ene | 19.80 | 1.45 | 1156 | 1320 | 34.78 | 4.06 | 0.12 | 2.17E−05 | 146 | 3 |
| 226 | (−)-Myrtenol | 21.07 | 1.41 | 1182 | 1308 | 38.72 | 9.39 | 0.24 | 1.79E−02 | 152 | 10 |
| 866 | Unknown | 24.29 | 1.20 | 1253 | 1308 | 1.79 | 0.25 | 0.14 | – | – | – |
| 290 | Cyclohexanone, 5-methyl-2-(1-methylethyl)-, cis- | 20.24 | 1.43 | 1166 | 1296 | 24.32 | 3.23 | 0.13 | 2.56E−01 | 154 | 7 |
| 643 | 2,4-Dodecadiene, (E,Z)- | 24.80 | 1.01 | 1265 | 1296 | 6.03 | 0.71 | 0.12 | 1.66E−01 | 166 | 5 |
| 166 | 2-Decene, 4-methyl-, (Z)- | 25.00 | 1.43 | 1269 | 1284 | 40.07 | 8.83 | 0.22 | 9.22E−01 | 196 | 5 |
| 651 | Megastigma-7(E),9,13-triene | 27.20 | 1.26 | 1318 | 1284 | 8.21 | 1.81 | 0.22 | 6.72E−02 | 176 | 3 |
| 247 | Benzene, (3-methyl-3-butenyl)- | 19.27 | 1.35 | 1145 | 1272 | 27.02 | 3.35 | 0.12 | 5.15E−01 | 146 | 2 |
| 671 | Trans-α-bisabolene | 37.80 | 1.39 | 1575 | 1272 | 2.42 | 2.16 | 0.89 | 7.87E−03 | 204 | 3 |
| 717 | Endo-7-Butyl-7-methoxybicyclo[4.1.0]hept-2-ene | 25.13 | 1.19 | 1272 | 1272 | 5.02 | 0.60 | 0.12 | 1.27E−01 | 180 | 3 |
| 394 | 2(5H)-Furanone, 5-ethyl- | 20.30 | 2.82 | 1168 | 1260 | 14.13 | 12.12 | 0.86 | 8.72E−02 | 112 | 12 |
| 69 | 2-Cyclopenten-1-one, 2,3-dimethyl- | 12.70 | 1.73 | 991 | 1248 | 114.34 | 24.54 | 0.21 | 1.33E+00 | 110 | 7 |
| 1069 | Unknown | 38.53 | 1.23 | 1593 | 1248 | 0.32 | 0.32 | 1.00 | – | – | – |
| 560 | Biphenylene, 1,2,3,6,7,8,8a,8b-octahydro-, trans- | 25.67 | 1.41 | 1284 | 1236 | 20.83 | 4.67 | 0.22 | 6.56E−03 | 160 | 3 |
| 82 | Cis-p-mentha-1(7),8-dien-2-ol | 20.60 | 1.43 | 1173 | 1224 | 59.99 | 14.30 | 0.24 | 1.52E−02 | 152 | 10 |
| 103 | 2-Propenal, 3-phenyl- | 18.73 | 1.45 | 1116 | 1224 | 92.35 | 13.32 | 0.14 | 2.65E−02 | 160 | 9 |
| 301 | Benzene, (1-methylbutyl)- | 20.53 | 1.31 | 1172 | 1224 | 19.45 | 2.27 | 0.12 | 6.96E−01 | 148 | 2 |
| 208* | 4-Methyl-1-indanone | 31.20 | 2.51 | 1410 | 1200 | 23.36 | 28.47 | 1.22 | 7.85E−03 | 146 | 7 |
| 458 | (E,E)-4,8,12-Trimethyl-1,3,7,11-tridecatetraene | 37.93 | 1.17 | 1578 | 1200 | 10.59 | 9.21 | 0.87 | 3.07E−03 | 218 | 5 |
| 593 | 2,5-Pyrrolidinedione, 1-ethyl- | 19.57 | 2.67 | 1152 | 1188 | 7.93 | 5.75 | 0.73 | 4.85E−02 | 127 | 17 |
| 783* | Naphthalene, 1,4,5-trimethyl- | 36.44 | 2.02 | 1541 | 1188 | 1.83 | 1.95 | 1.07 | 3.64E−03 | 170 | 1 |
| 31 | Benzenepropanenitrile | 24.40 | 2.57 | 1256 | 1176 | 122.60 | 99.50 | 0.81 | 1.13E−02 | 131 | 14 |
| 73 | Benzofuran, 4,7-dimethyl- | 23.07 | 1.71 | 1226 | 1176 | 87.81 | 18.05 | 0.21 | 1.88E−01 | 146 | 18 |
| 446* | 2,3-Dimethylenebutane-1,4-diacetate | 24.60 | 2.82 | 1260 | 1176 | 17.26 | 17.56 | 1.02 | 5.42E−03 | 198 | 11 |
| 838 | Unknown | 22.66 | 1.17 | 1218 | 1176 | 2.50 | 0.26 | 0.10 | – | – | – |
| 756 | Unknown | 22.80 | 1.09 | 1221 | 1152 | 8.22 | 0.64 | 0.08 | – | – | – |
| 570 | Naphthalene, 1,2,3,4-tetrahydro-1,8-dimethyl- | 26.14 | 1.51 | 1294 | 1140 | 13.19 | 3.22 | 0.24 | 5.48E−02 | 160 | 1 |
| 685* | 1H-Indole, 3-methyl- | 31.43 | 2.61 | 1415 | 1140 | 3.91 | 5.13 | 1.31 | 1.53E−02 | 131 | 1 |
| 924 | 1H-3a,7-Methanoazulene, octahydro-1,4,9,9-tetramethyl- | 25.33 | 1.10 | 1276 | 1140 | 3.54 | 0.34 | 0.10 | 1.89E−02 | 206 | 3 |
| 133 | Pyridine, 3-ethyl- | 11.03 | 1.51 | 952 | 1128 | 66.19 | 7.50 | 0.11 | 2.42E+00 | 107 | 8 |
| 331 | 1,2-Propanediol, 2-acetate | 8.47 | 1.24 | 891 | 1128 | 54.27 | 5.44 | 0.10 | 1.42E−01 | 118 | 11 |
| 835 | 10,12-Octadecadiynoic acid | 36.84 | 1.49 | 1549 | 1128 | 2.13 | 1.83 | 0.86 | 7.31E−09 | 276 | 15 |
| 615 | Unknown | 25.85 | 2.40 | 1287 | 1116 | 9.32 | 8.13 | 0.87 | – | – | – |

| | | | | | | | | | | | |
|---|---|---|---|---|---|---|---|---|---|---|---|
| 702 | 3-Tridecene, (E)- | 27.07 | 0.87 | 1315 | 1116 | 4.48 | 0.91 | 0.20 | 9.03E−02 | 180 | 5 |
| 23 | Pyridine, 3-ethenyl- | 11.60 | 1.60 | 965 | 1104 | 230.74 | 35.30 | 0.15 | 9.03E−02 | 105 | 8 |
| 190 | 1H-Indene, 2,3-dihydro-1,3-dimethyl- | 21.67 | 1.46 | 1194 | 1104 | 62.28 | 11.83 | 0.19 | 3.05E−01 | 146 | 1 |
| 723 | Benzene, 1,4-dimethyl-2-(2-methylpropyl)- | 22.06 | 1.23 | 1204 | 1104 | 2.84 | 0.22 | 0.08 | 1.51E−01 | 162 | 2 |
| 900 | Unknown | 25.12 | 1.02 | 1272 | 1104 | 3.27 | 0.36 | 0.11 | – | – | – |
| 91 | 1H-Indene, 1,1-dimethyl- | 25.27 | 1.73 | 1276 | 1092 | 81.57 | 22.85 | 0.28 | 3.39E−01 | 144 | 1 |
| 856 | Unknown | 24.57 | 1.03 | 1260 | 1092 | 6.89 | 0.95 | 0.14 | – | – | – |
| 384 | Unknown | 18.99 | 1.58 | 1139 | 1068 | 8.77 | 1.36 | 0.16 | – | – | – |
| 715 | Unknown | 26.87 | 1.36 | 1311 | 1068 | 11.97 | 2.33 | 0.19 | – | – | – |
| 860 | Unknown | 37.93 | 1.51 | 1578 | 1068 | 2.25 | 2.16 | 0.96 | – | – | – |
| 930 | Unknown | 26.73 | 1.02 | 1308 | 1068 | 1.99 | 0.34 | 0.17 | – | – | – |
| 823 | Unknown | 28.67 | 1.12 | 1353 | 1056 | 1.77 | 0.37 | 0.21 | – | – | – |
| 102 | (E)-1-Phenyl-1-butene | 17.81 | 1.68 | 1134 | 1044 | 57.25 | 6.31 | 0.11 | 8.05E−01 | 132 | 2 |
| 191 | Benzene, (2-methyl-1-propenyl)- | 19.00 | 1.47 | 1139 | 1044 | 46.11 | 3.02 | 0.07 | 8.49E−01 | 132 | 2 |
| 494 | 3,4-Pyridinedimethanol, 6-methyl- | 15.93 | 1.45 | 1071 | 1044 | 5.84 | 0.63 | 0.11 | 5.16E−05 | 153 | 10 |
| 379 | Benzene, 4-hexenyl- | 24.53 | 1.40 | 1259 | 1032 | 8.61 | 1.79 | 0.21 | 1.19E−01 | 160 | 2 |
| 500 | (1-Methylpenta-2,4-dienyl)benzene | 25.61 | 1.61 | 1282 | 1032 | 9.61 | 2.63 | 0.27 | 0 | 158 | 2 |
| 35 | 1H-Inden-1-one, 2,3-dihydro- | 26.30 | 2.59 | 1299 | 1020 | 98.15 | 77.65 | 0.79 | 3.11E−02 | 132 | 7 |
| 613 | Ethanone, 1-(2-furanyl)- | 21.11 | 1.27 | 1185 | 1020 | 5.14 | 0.36 | 0.07 | 7.72E−01 | 110 | 18 |
| 41 | 1H-Indene | 15.00 | 1.62 | 1048 | 1008 | 154.86 | 18.55 | 0.12 | 7.72E−01 | 116 | 1 |
| 293 | Benzene, 2-ethenyl-1,4-dimethyl- | 17.60 | 1.43 | 1110 | 996 | 30.86 | 2.05 | 0.07 | 6.28E−01 | 132 | 2 |
| 433 | 2-Decanone | 21.79 | 1.28 | 1199 | 996 | 22.55 | 2.31 | 0.10 | 2.48E−01 | 156 | 7 |
| 558 | 6-Methyl-1,2,3,4-tetrahydroquinoline | 31.27 | 2.25 | 1410 | 996 | 7.70 | 7.24 | 0.94 | 9.82E−03 | 147 | 16 |
| 626 | 1H-Indene, 2,3-dihydro-1,1,5,6-tetramethyl- | 27.60 | 1.34 | 1327 | 996 | 7.60 | 1.75 | 0.23 | 6.85E−02 | 174 | 1 |
| 826 | 4-(2-Methylcyclohex-1-enyl)-but-2-enal | 21.12 | 0.99 | 1185 | 996 | 4.28 | 0.11 | 0.03 | 9.99E−03 | 164 | 9 |
| 841 | Unknown | 26.66 | 1.36 | 1306 | 996 | 3.31 | 0.69 | 0.21 | – | – | – |
| 927 | 1-Dodecyne | 23.53 | 0.98 | 1237 | 996 | 1.92 | 0.17 | 0.09 | 2.22E−01 | 166 | 4 |
| 620 | Unknown | 25.40 | 1.43 | 1278 | 984 | 5.77 | 1.24 | 0.21 | – | – | – |
| 164 | Pyrazine, 2-ethyl-6-methyl- | 12.87 | 1.47 | 996 | 972 | 18.49 | 1.05 | 0.06 | 1.98E+00 | 122 | 8 |
| 176 | Benzene, 1-methoxy-4-methyl- | 13.87 | 1.53 | 1020 | 972 | 40.95 | 1.95 | 0.05 | 1.65E+00 | 122 | 2 |
| 225 | Benzene, 1-ethyl-4-methoxy- | 18.27 | 1.60 | 1124 | 972 | 55.68 | 7.40 | 0.13 | 5.86E−01 | 136 | 2 |
| 576 | Benzene, 1,2,4-triethyl- | 22.51 | 1.30 | 1215 | 972 | 13.23 | 1.36 | 0.10 | 1.88E−01 | 162 | 2 |
| 754 | Unknown | 27.78 | 1.13 | 1332 | 972 | 4.24 | 1.03 | 0.24 | – | – | – |
| 802* | Unknown | 35.10 | 2.49 | 1505 | 972 | 0.79 | 1.33 | 1.68 | – | – | – |
| 20 | 5-Methyl furfural | 11.34 | 1.80 | 959 | 960 | 183.17 | 48.24 | 0.26 | 6.44E−01 | 110 | 9 |
| 250 | Benzene, 1,2,4,5-tetramethyl- | 18.40 | 1.36 | 1127 | 960 | 28.69 | 2.47 | 0.09 | 6.96E−01 | 134 | 2 |
| 484 | 4-Tridecen-1-ol, acetate, (E)- | 27.67 | 0.94 | 1329 | 960 | 12.10 | 2.77 | 0.23 | 3.34E−03 | 240 | 11 |
| 765 | Unknown | 31.44 | 2.41 | 1415 | 960 | 1.79 | 1.77 | 0.99 | – | – | – |
| 776 | Unknown | 27.68 | 1.24 | 1329 | 960 | 5.56 | 1.25 | 0.22 | – | – | – |
| 58 | 2-Cyclopenten-1-one, 3-(1-methylethyl)- | 17.56 | 1.81 | 1110 | 948 | 142.17 | 33.34 | 0.23 | 1.43E−01 | 124 | 7 |
| 122 | 1H-Indene, 2,3-dihydro-4-methyl- | 19.40 | 1.52 | 1148 | 948 | 27.38 | 3.86 | 0.14 | 3.46E−01 | 132 | 1 |
| 248 | 2-Cyclohexen-1-one, 4-ethyl-4-methyl- | 18.40 | 1.56 | 1127 | 948 | 24.16 | 3.17 | 0.13 | 3.11E−01 | 138 | 7 |
| 509 | Naphthalene, 1,2,3,4-tetrahydro-1,5-dimethyl- | 26.43 | 1.53 | 1302 | 948 | 25.07 | 7.25 | 0.29 | 5.64E−02 | 160 | 1 |
| 837 | Unknown | 28.69 | 1.18 | 1353 | 948 | 5.46 | 0.95 | 0.17 | – | – | – |
| 884 | α-Calacorene | 36.87 | 1.66 | 1551 | 948 | 3.59 | 3.14 | 0.87 | 3.74E−03 | 172 | 3 |
| 1160* | Unknown | 32.37 | 3.13 | 1438 | 948 | 0.36 | 0.43 | 1.19 | – | – | – |

Table 2 (*Continued*)

| Blob ID | Area name | $^1t_R$ mean [min] | $^2t_R$ mean [s] | LRI | *F* | Peak volume mean (A) $\times 10^6$ | Peak volume mean (B) $\times 10^6$ | Peak volume mean ratio | Vapor pressure at 298 K [Torr] | MW | Chemical class[a] | |
|---|---|---|---|---|---|---|---|---|---|---|---|---|
| 161 | Benzonitrile, 2-methyl- | 18.00 | 2.06 | 1118 | 936 | 34.65 | 8.11 | 0.23 | 2.43E−01 | 117 | 14 | |
| 209 | 2-Cyclopenten-1-one, 3,4-dimethyl- | 10.53 | 1.45 | 940 | 936 | 59.10 | 5.37 | 0.09 | 1.69E+00 | 110 | 7 | |
| 241 | 2-Norcaranone, 3-methyl- | 16.13 | 1.67 | 1076 | 936 | 31.26 | 5.18 | 0.17 | 4.97E−01 | 124 | 7 | |
| 843 | p-Menthone | 25.70 | 2.90 | 1285 | 936 | 8.14 | 7.28 | 0.89 | 2.56E−01 | 154 | 7 | |
| 422 | Benzene, 2-ethenyl-1,3,5-trimethyl- | 22.79 | 1.49 | 1221 | 924 | 32.80 | 5.76 | 0.18 | 3.29E−01 | 146 | 2 | |
| 649 | Unknown | 27.20 | 1.29 | 1318 | 924 | 6.66 | 1.75 | 0.26 | – | – | – | |
| 937 | Isolongifolene, 4,5,9,10-dehydro- | 37.95 | 1.72 | 1580 | 924 | 0.87 | 0.78 | 0.90 | 2.62E−02 | 200 | 3 | |
| 281 | Unknown | 24.67 | 1.39 | 1262 | 912 | 33.92 | 9.89 | 0.29 | – | – | – | |
| 527 | Benzene, 1,3-dimethyl-5-(1-methylethyl)- | 22.46 | 1.42 | 1213 | 912 | 15.86 | 2.62 | 0.17 | 6.33E−01 | 148 | 2 | |
| 610 | 3,8-Dimethyl-1-cyclobutene | 26.33 | 2.44 | 1299 | 912 | 4.60 | 3.64 | 0.79 | 2.48E+02 | 134 | 5 | |
| 1260 | Unknown | 40.66 | 1.33 | 1650 | 912 | 0.46 | 0.43 | 0.93 | – | – | – | |

* Compounds which were better removed by a classic cellulose acetate filter.

[a] Chemical classes: 1, polycyclic aromatic hydrocarbons (PAHs); 2, monocyclic aromatic hydrocarbons; 3, alicyclic hydrocarbons; 4, alkynes; 5, alkenes; 6, alkanes; 7, ketones; 8, monocyclic six-membered *N*-containing ring compounds; 9, aldehydes; 10, alcohols; 11, esters; 12, lactones; 13, phenols; 14, nitriles; 15, carboxylic acids; 16, aza-arenes; 17, imides; 18, ethers.

### 3.3. Pixel-based data processing and principal component analysis

The pixel-based software package (GC Image™) was used for alignment and comparison of chromatograms from the 12 replicates of cigarette type A and 12 replicates of cigarette type B (a total of 24 runs were conducted). Samples were preprocessed by mean of background correction, blob detection, and phase shift. The alignment was based on reliable peaks that could be detected and matched in all samples. Then, a cumulative chromatogram was created by combining all chromatograms into a single image. Such an image reflected all of the constituents present in all samples. Each peak present in this image was delineated, forming regions that were recorded and used to create a template. For each of the peaks, the template matrix recorded retention times in both dimensions ($^1t_R$ and $^2t_R$) and a rule expressed in Computer Language for Identifying Chemicals (CLIC) [48] that specifies the reference mass spectrum in the template as well as the required mass spectral match factor to be reached when in use. After a final set of manual cleaning for column bleeding signals, artifacts, and peak tailing-related hits, a final set of 1170 regions was created in the template. Each of the single HS-SPME GC × GC TOFMS chromatograms generated by the replicated analyses of both types A and B cigarettes were mapped back to this template and each region defined a feature for each chromatogram. A large matrix (24 × 1170) of data containing the relative percent responses of peak areas for each of the 1170 regions of the 24 mainstream smoke PP samples was created and submitted to principal component analysis (PCA) with mean-centering pretreatment. Fig. 4 (top) shows the corresponding PC1 vs. PC2 *score* plot. These two principal components summarize the relationships among the samples and account for more variation in the data set than any other pair of components with PC1 describing 98% of the explained variance. This clearly demonstrated the efficiency of the multivariate data processing approach for the segregation of PP smoke components from the two cigarette types based on their difference in terms of filter construction.

Furthermore, when considering the *loadings* to interpret the patterns seen in the *score* plot, and focusing only on compounds representative for each type of cigarettes (further to the right for the type A and further to the left for the type B in Fig. 4 bottom) we can observe that compounds characteristic for the cellulose acetate filter type A cigarettes are more volatile and less polar than compounds specific for the active carbon/cellulose acetate filtered type B (Fig. 5).

### 3.4. Statistical comparison using pairwise Fisher ratio

Compared to the PCA approach, this statistical comparison relied on the creation of different classes of samples prior to data processing. Contrary to unsupervised PCA analysis, which is more likely to fail for datasets with high portions of within-class variations, the supervised Fisher ratio (*F*) is well suited for such sample profiles. This type of analysis differentiates the fragments of the sample profile that contain class-to-class variations from the fragments of the sample that contain within-class variations, and can be applied to discover the unknown chemical differences among known classes of complex samples [43]. Fisher ratios were calculated for all of the 1170 regions of the template for the 12 GC × GC chromatogram replicates available for each of the two classes of cigarettes. For each compound region, a mean volume value was calculated for both classes prior to *F* calculation and normalized against the sum of all volumes of the class so that it was based on a percent response. Fig. 6A shows the two-dimensional (mean $^1t_R$ ($^1t$) vs. mean $^2t_R$ ($^2t$)) Fisher ratio plot for percent responses of compounds detected in the 24 aligned GC × GC chromatograms. Bubbles represent the Fisher ratio values for detected analytes;

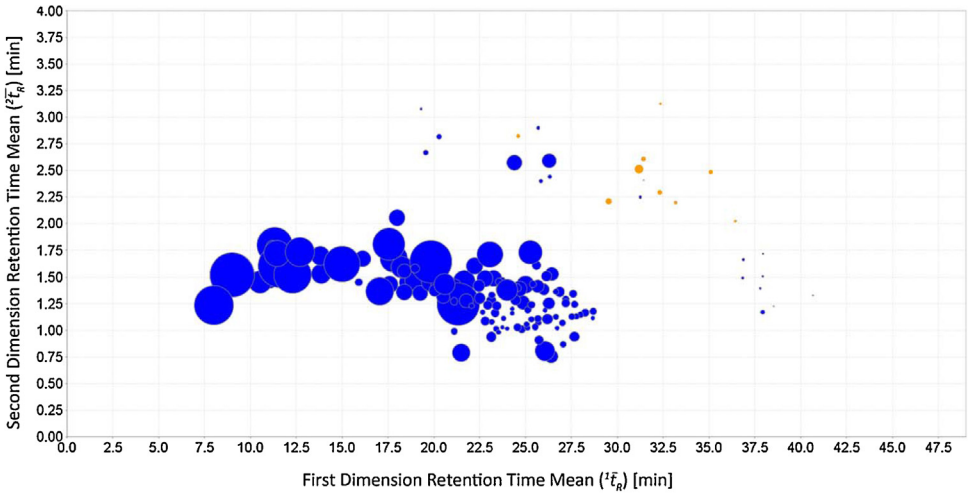


**Fig. 7.** Two-dimensional plot showing differences in peak volume means for the selected 143 compounds. Mean differences are proportional to the size of the bubbles; positive differences are shown as blue bubbles while negative as orange ones. (For interpretation of the references to color in text, the reader is referred to the web version of the article.)

the bigger the bubble the higher the *F*, thus the greater the differences between the two classes. The value of such a plot is that it allows direct appreciation of how the compounds responsible for the class separation are located in the chromatographic space. Such a link with the chemical elution logic allows the zones that are particularly distinctive to be distinguished. Although the roof-tile effect, where peaks belonging to homologous series are positioned along lines on the retention plane, is not as strong as in petrochemical samples, it is possible to draw some conclusions regarding the chemical character of the cigarette smoke components resulting from the differences in the cigarette filter construction. In the present case, differences are localized where moderately polar and highly polar compounds with higher molecular weights elute, such as monocyclic and polycyclic aromatics.

Calculated Fisher ratio values for percent responses ranged between $1.92 \times 10^{-4}$ and 6648. Statistically significant differences are observed when calculated value of *F* exceeds the critical value ($F_{crit}$), the same way it is done in one-way ANOVA. In this case, for 12 samples in each class and significance level $\alpha = 0.01$, the critical value $F_{crit}$ was 7.95. For the analysis of compounds from cigarettes A and B, statistically significant differences were observed for 1101 analytes, which is nearly 94%. In order to focus our efforts on compounds that exhibited the greatest class-to-class variation, we chose to apply a threshold value of 900. A set of 143 compounds selected in this way showed the biggest influence on the differences between the two classes of cigarettes and included 13% of the significantly different features (Fig. 6B).

Fisher ratio analysis is very useful to identify the major compounds responsible for the differences between 2 classes, especially, for example, in the case of on/off responses to illnesses [49]. However, it gives no information regarding changes in the concentration of the analytes present in several classes. It was nevertheless possible to specifically reprocess the data for the 143 compounds exhibiting *F* values greater than 900 to examine the separate peak volume means and thereby calculate the difference for each compound in both classes. In Fig. 7, each bubble represents a difference in peak volume means for classes A and B, and the size of the bubble is proportional to that difference. For 134 of the 143 features, this difference was positive (showed as blue bubbles in Fig. 7). This showed that the use of activated carbon in the filter design resulted in a reduction of the relative concentration of these analytes in the mainstream smoke PP. For the nine remaining compounds, characterized by higher molecular weights and eluting at the end of a chromatographic run (showed as orange bubbles in Fig. 7), negative values for peak volume means were observed. These values, although much smaller than for the positive values for peak volume means, suggest that for these analytes a classical cellulose acetate filter had a more efficient trapping effect than the charcoal filter. Table 2 lists the above mentioned tentatively identified compounds (based on mass spectral similarities and LRIs, when available) in a descending order of Fisher ratio value; their vapor pressure (VP) values at 25 °C, peak volume means for both classes of cigarettes, and their ratios, and molecular weights are also shown. Whilst the purity of the GC × GC TOFMS spectra is generally high, leading to good quality library matches, 38 from the 143 peaks remained unassigned because they were not present among the 680,000 entries of the libraries that were used. Such a situation is common, as up to 70% of peaks in a typical GC/MS analysis of a plant extract remain unidentified after library searches [50]. The use of high accuracy MS analyzers would be of significant value in such cases of lack of identification.

Among the compounds identified as different between the two cigarettes, the majority were hydrocarbons (monocyclic aromatic – 25, polycyclic aromatic – 13, alkenes – 12, alicyclics – 9, alkynes – 2, and alkanes – 1), while the other major classes of compounds are ketones (11), monocyclic six-membered *N*-containing compounds (6), alcohols (5), aldehydes (5), esters (4), lactones (3), nitriles (2), phenols (2), ethers (2), carboxylic acids (1), aza-arenes (1), and imides (1). Analytes that were better removed by a classic cellulose acetate filter possessed molecular weight in the range of 131 and 170; 3 of them were PAHs, 2 were unknown, while the remaining ones, with one member per class, belong to monocyclic six-membered *N*-containing compounds, phenols, ketones, and esters.

We attempted to explain the observed differences in chemical profiles of the two smoke samples on the basis of the physical properties of individual smoke constituents. However, despite our attempts, we could not identify any simple relationship between ratios of peak volumes of selected compounds (column 9 of Table 2) and their vapor pressure values (column 10 of Table 2). Generally, compounds that were better removed by a cellulose acetate filter had vapor pressure values below 0.043 at 25 °C; however, other compounds, with similar or lower values, were better removed by an active carbon filter. Also, compounds with high and low peak volume ratios were characterized by similar VP values. Relating other chemical factors, such as molecular weights (MW), boiling points (seen as elution in the first dimension), or polarity, to the observed differences in the relative yields also failed to identify a

clear reason for differences between the smoke samples. A further investigation by means of a multivariate analysis of possible physicochemical properties would be necessary to explain the processes occurring during PP filtration and factors affecting it.

## 4. Conclusions

A method involving headspace solid-phase microextraction and GC × GC TOFMS was developed for the analysis of mainstream cigarette smoke particular matter from two types of cigarettes differing in filter construction. Polyacrylate SPME fiber was chosen over other five types of fibers for the analysis while extraction conditions were selected using an experimental design approach. The strategy of multivariate experimental design made possible the identification of experimental conditions (extraction time and extraction temperature) for the headspace SPME sampling method using an efficient experimental approach. Maximized desirability was achieved at an extraction temperature of 40 °C and extraction time of 15 min. Optimized conditions were used to perform 12 replicate analyses of each cigarette type, followed by automated detection and recognition of peak patterns in individual chromatograms, selection of reliable peaks to perform alignment of all samples, and creation of a cumulative template to contain region features. These areas were used for cross-sample comparison. Fisher ratio analysis allowed selection of 143 compounds (with *F* values over 900) having the biggest influence on the differences between two types of cigarettes, nearly 60% of which (excluding unknowns) belonged to hydrocarbons. Application of active carbon in a filter design resulted in a reduction of 134 of these analytes while nine were better removed from the mainstream smoke using a classical cellulose acetate filter. Principal component analysis allowed grouping tendencies to be identified and clear differentiation between the two types of cigarettes. The use of high-resolution mass spectrometry (HRMS) for precise elemental analysis might be necessary to identify unknown compounds.

## Acknowledgments

We wish to thank Restek Corp. and SGE International for providing us with consumables and Gerstel Japan for the license of Aroma Office $^{2}$D.

## References

[1] A. Rodgman, T.A. Perfetti, The Chemical Components of Tobacco and Tobacco Smoke, CRC Press, Boca Raton, 2009.
[2] L.A. Clunes, A. Bridges, N. Alexis, R. Tarran, In vivo versus in vitro airway surface liquid nicotine levels following cigarette smoke exposure, J. Anal. Toxicol. 32 (2008) 201–207.
[3] A. Rodgman, T.A. Perfetti, The Chemical Components of Tobacco and Tobacco Smoke, second edition, CRC Press, Boca Raton, 2013.
[4] H. Wakeham, in: I. Schmeltz (Ed.), 162nd National Meeting, American Chemical Society, Plenum Press, Washington, DC, 1971, p. 1.
[5] S.M. Charles, S.A. Batterman, C. Jia, Composition and emissions of VOCs in main- and side-stream smoke of research cigarettes, Atmos. Environ. 41 (2007) 5371–5384.
[6] S.M. Charles, C. Jia, S.A. Batterman, C. Godwin, VOC and particulate emissions from commercial cigarettes: analysis of 2,5-DMF as an ETS tracer, Environ. Sci. Technol. 42 (2008) 1324–1331.
[7] Q. Ye, Development of solid-phase microextraction followed by gas chromatography–mass spectrometry for rapid analysis of volatile organic chemicals in mainstream cigarette smoke, J. Chromatogr. A 1213 (2008) 239–244.
[8] G.M. Polzin, R.E. Kosa-Maines, D.L. Ashley, C.H. Watson, Analysis of volatile organic compounds in mainstream cigarette smoke, Environ. Sci. Technol. 41 (2007) 1297–1302.
[9] Y.S. Ding, X.J. Yan, R.B. Jain, E. Lopp, A. Tavakoli, G.M. Polzin, S.B. Stanfill, D.L. Ashley, C.H. Watson, Determination of 14 polycyclic aromatic hydrocarbons in mainstream smoke from U.S. brand and non-U.S. brand cigarettes, Environ. Sci. Technol. 40 (2006) 1133–1138.
[10] G. Gmeiner, G. Stehlik, H. Tausch, Determination of seventeen polycyclic aromatic hydrocarbons in tobacco smoke condensate, J. Chromatogr. A 767 (1997) 163–169.
[11] J. Li, Y.L. Feng, C.J. Xie, J. Huang, J.Z. Yu, J.L. Feng, G.Y. Sheng, J.M. Fu, M.H. Wu, Determination of gaseous carbonyl compounds by their pentafluorophenyl hydrazones with gas chromatography/mass spectrometry, Anal. Chim. Acta 635 (2009) 84–93.
[12] X. Pang, A.C. Lewis, Carbonyl compounds in gas and particle phases of mainstream cigarette smoke, Sci. Total Environ. 409 (2011) 5000–5009.
[13] N.P. Kulshreshtha, S.C. Moldoveanu, Analysis of pyridines in mainstream cigarette smoke, J. Chromatogr. A 985 (2003) 303–312.
[14] S.C. Moldoveanu, M. Kiser, Gas chromatography/mass spectrometry versus liquid chromatography/fluorescence detection in the analysis of phenols in mainstream cigarette smoke, J. Chromatogr. A 1141 (2007) 90–97.
[15] J. Cai, B. Liu, P. Lin, Q. Su, Fast analysis of nicotine related alkaloids in tobacco and cigarette smoke by megabore capillary gas chromatography, J. Chromatogr. A 1017 (2003) 187–193.
[16] M. Bao, P. Joza, W.S. Rickert, J.H. Lauterbach, An improved headspace solid-phase microextraction method for the analysis of free-base nicotine in particulate phase of mainstream cigarette smoke, Anal. Chim. Acta 663 (2010) 49–54.
[17] M. Adahchour, J. Beens, R.J.J. Vreuls, U.A.T. Brinkman, Recent developments in comprehensive two-dimensional gas chromatography (GC × GC) III. Applications for petrochemicals and organohalogens, Trends Anal. Chem. 25 (2006) 726–741.
[18] M. Adahchour, J. Beens, R.J.J. Vreuls, U.A.T. Brinkman, Recent developments in comprehensive two-dimensional gas chromatography (GC × GC) IV. Further applications, conclusions and perspectives, Trends Anal. Chem. 25 (2006) 821–840.
[19] M. Brokl, L. Bishop, C.G. Wright, C. Liu, K. McAdam, J.-F. Focant, Analysis of mainstream tobacco smoke particulate phase using comprehensive two-dimensional gas chromatography time-of-flight mass spectrometry, J. Sep. Sci. 36 (2013) 1037–1044.
[20] S. Stadler, P.-H. Stefanuto, M. Brokl, S.L. Forbes, J.-F. Focant, Characterization of volatile organic compounds from human analogue decomposition using thermal desorption coupled to comprehensive two-dimensional gas chromatography–time-of-flight mass spectrometry, Anal. Chem. 85 (2012) 998–1005.
[21] J. Dallüge, L.L.P. van Stee, X. Xu, J. Williams, J. Beens, R.J.J. Vreuls, U.A.T. Brinkman, Unravelling the composition of very complex mixtures by GC × GC TOFMS cigarette smoke, J. Chromatogr. A 974 (2002) 169–184.
[22] X. Lu, M. Zhao, H. Kong, J. Cai, J. Wu, M. Wu, R. Hua, J. Liu, G. Xu, Characterization of cigarette smoke condensates by comprehensive two-dimensional gas chromatography/time-of-flight mass spectrometry (GC × GC/TOFMS). Part 2: basic fraction, J. Sep. Sci. 27 (2004) 101–109.
[23] X. Lu, J. Cai, H. Kong, M. Wu, R. Hua, M. Zhao, J. Liu, G. Xu, Analysis of cigarette smoke condensates by comprehensive two-dimensional gas chromatography/time-of-flight mass spectrometry I acidic fraction, Anal. Chem. 75 (2003) 4441–4451.
[24] X. Lu, M. Zhao, H. Kong, J. Cai, J. Wu, M. Wu, R. Hua, J. Liu, G. Xu, Characterization of complex hydrocarbons in cigarette smoke condensate by gas chromatography–mass spectrometry and comprehensive two-dimensional gas chromatography–time-of-flight mass spectrometry, J. Chromatogr. A 1043 (2004) 265–273.
[25] J.-F. Focant, A. Sjödin, W.E. Turner, D.G. Patterson, Measurement of selected polybrominated diphenyl ethers, polybrominated and polychlorinated biphenyls, and organochlorine pesticides in human serum and milk using comprehensive two-dimensional gas chromatography isotope dilution time-of-flight mass spectrometry, Anal. Chem. 76 (2004) 6313–6320.
[26] J. Pawliszyn, in: J. Pawliszyn (Ed.), Handbook of Solid Phase Microextraction, Elsevier, Oxford, 2012, pp. 13–59.
[27] C.L. Arthur, J. Pawliszyn, Solid phase microextraction with thermal desorption using fused silica optical fibers, Anal. Chem. 62 (1990) 2145–2148.
[28] L. Kudlejova, S. Risticevic, J. Pawliszyn (Eds.), Handbook of Solid Phase Microextraction, Elsevier, Oxford, 2012, pp. 291–334.
[29] H. Lord, B. Bojko, in: J. Pawliszyn (Ed.), Handbook of Solid Phase Microextraction, Elsevier, Oxford, 2012, pp. 335–382.
[30] G. Ouyang, in: J. Pawliszyn (Ed.), Handbook of Solid Phase Microextraction, Elsevier, Oxford, 2012, pp. 251–290.
[31] T.J. Clark, J.E. Bunch, Quantitative determination of phenols in mainstream smoke with solid-phase microextraction-gas chromatography – selected ion monitoring mass spectrometry, J. Chromatogr. Sci. 34 (1996) 272–275.
[32] T.J. Clark, J.E. Bunch, Qualitative and quantitative analysis of flavor additives on tobacco products using SPME–GC–mass spectroscopy, J. Agric. Food Chem. 45 (1997) 844–849.
[33] S.B. Stanfill, D.L. Ashley, Solid phase microextraction of alkenylbenzenes and other flavor-related compounds from tobacco for analysis by selected ion monitoring gas chromatography–mass spectrometry, J. Chromatogr. A 858 (1999) 79–89.
[34] C. Merckel, F. Pragst, A. Ratzinger, B. Aebi, W. Bernhard, F. Sporkert, Application of headspace solid phase microextraction to qualitative and quantitative analysis of tobacco additives in cigarettes, J. Chromatogr. A 1116 (2006) 10–19.
[35] S.S. Yang, C.B. Huang, I. Smetena, Optimization of headspace sampling using solid-phase microextraction for volatile components in tobacco, J. Chromatogr. A 942 (2002) 33–39.

[36] S.S. Yang, I. Smetena, Determination of tobacco alkaloids using solid phase microextraction and GC-NPD, Chromatographia 47 (1998) 443–448.
[37] C.H. Watson, D.L. Ashley, Quantitative analysis of acetates in cigarette tobacco using solid-phase microextraction and gas chromatography–mass spectrometry, J. Chromatogr. Sci. 38 (2000) 137–144.
[38] H. Lin, Q. Ye, C. Deng, X. Zhang, Field analysis of acetaldehyde in mainstream tobacco smoke using solid-phase microextraction and a portable gas chromatograph, J. Chromatogr. A 1198–1199 (2008) 34–37.
[39] C.H. Watson, J.S. Trommel, D.L. Ashley, Solid-phase microextraction-based approach to determine free-base nicotine in trapped mainstream cigarette smoke total particulate matter, J. Agric. Food Chem. 52 (2004) 7240–7245.
[40] G. Pieraccini, S. Furlanetto, S. Orlandini, G. Bartolucci, I. Giannini, S. Pinzauti, G. Moneti, Identification and determination of mainstream and sidestream smoke components in different brands and types of cigarettes by means of solid-phase microextraction – gas chromatography–mass spectrometry, J. Chromatogr. A 1180 (2008) 138–150.
[41] S.L.C. Ferreira, R.E. Bruns, E.G.P. da Silva, W.N.L. dos Santos, C.M. Quintella, J.M. David, J.B. de Andrade, M.C. Breitkreitz, I.C.S.F. Jardim, B.B. Neto, Statistical designs and response surface techniques for the optimization of chromatographic systems, J. Chromatogr. A 1158 (2007) 2–14.
[42] P. Branton, K. McAdam, M. Duke, C. Liu, M. Curle, M. Mola, C. Proctor, R. Bradley, Use of classical adsorption theory to understand the dynamic filtration of volatile toxicants in cigarette smoke by active carbons, Adsorpt. Sci. Technol. 29 (2011) 117–138.
[43] K.M. Pierce, J.C. Hoggard, J.L. Hope, P.M. Rainey, A.N. Hoofnagle, R.M. Jack, B.W. Wright, R.E. Synovec, Fisher ratio method applied to third-order separation data to identify significant chemical components of metabolite extracts, Anal. Chem. 78 (2006) 5068–5075.
[44] ISO 3402, Tobacco and Tobacco Products – Atmosphere for Conditioning and Testing, International Organization for Standardization, Geneva, 1999.
[45] ISO 3308, Routine Analytical Smoking Machine – Definition and Standard Conditions, International Organization for Standardization, Geneva, 2000.
[46] H. Martens, T. Naes, Multivariate Calibration, John Wiley & Sons, Ltd., Chichester, 1991.
[47] R.E. Shirey, in: J. Pawliszyn (Ed.), Handbook of Solid Phase Microextraction, Elsevier, Oxford, 2012, pp. 99–133.
[48] S.E. Reichenbach, V. Kottapalli, M. Ni, A. Visvanathan, Computer language for identifying chemicals with comprehensive two-dimensional gas chromatography and mass spectrometry, J. Chromatogr. A 1071 (2005) 263–269.
[49] A.C. Beckstrom, E.M. Humston, L.R. Snyder, R.E. Synovec, S.E. Juul, Application of comprehensive two-dimensional gas chromatography with time-of-flight mass spectrometry method to identify potential biomarkers of perinatal asphyxia in a non-human primate model, J. Chromatogr. A 1218 (2011) 1899–1906.
[50] R.J. Bino, R.D. Hall, O. Fiehn, J. Kopka, K. Saito, J. Draper, B.J. Nikolau, P. Mendes, U. Roessner-Tunali, M.H. Beale, R.N. Trethewey, B.M. Lange, E.S. Wurtele, L.W. Sumner, Potential of metabolomics as a functional genomics tool, Trends Plant Sci. 9 (2004) 418–425.